8-2017

MULTIPLE PATH PARTICLE DOSIMETRY FOR PREDICTION OF MOUSE LUNG DEPOSITION OF NANOAEROSOL PARTICLES

Mohammed Ali

The University of Texas at Tyler, mohammedali@uttyler.edu

Recommended Citation

MULTIPLE PATH PARTICLE DOSIMETRY FOR PREDICTION OF MOUSE LUNG DEPOSITION OF NANOAEROSOL PARTICLES

M. Ali

Department of Technology,
The University of Texas at Tyler, Longview, Texas 75605, USA

B. W. Gutting, M. L. van Hoek

School of Systems Biology
George Mason University, Manassas, Virginia 20110, USA

ABSTRACT

Nanoaerosolized particle (dia.<200 nm) antibiotic inhalation therapy was tested to treat pneumonic tularemia in mice caused by Francisellanovicida infection. Very limited experimental techniques are available to properly estimate inhaled doses and distribution of the drug inside the mouse lungs. To overcome this problem, computational simulation of particle deposition based on the Multiple Path Particle Dosimetry (MPPD) model was employed to simulate in vivo experimental conditions which included nasal breathing with whole body exposure to the antibiotic in the form of nano-aerosolized medicine. The deposition results were compared with several in vivo experimental data reported in literature; and satisfactory agreements were found. Comparing with in vivo experimental data, regional deposition results are very close with ±10-15% variations. After testing application of the MPPD model, the total inhaled doses of levofloxacin encapsulated into nanoliposomes were estimated which take into account distribution of sizes of nanoaersol particles. Thus, we have demonstrated that MPPD can be used to model the deposition of nanoaerosol particles in mice.

Key words: Nanoaerosol Particles, BALB/c mice, lung dosimetry, MPPD.

1. INTRODUCTION

Present knowledge reveals that the nanoparticle (NP) (an object with at least one dimension less than 100 nm) and ultrafine particle (UFP) (100 nm <dia.< 1000 nm) are highly effective in deep lung and/or alveolar penetration [1-4]. The key factors that contribute to the

effectiveness of NPs and UFPs transport and deposition are still not clear; however, literature suggests that simultaneous actions of their mass, number and surface area concentrations are important factors [5,6].

Lung delivery of nebulized liposomal Amikacin has been demonstrated success in reducing Pseudomonas infection in the cystic fibrosis human lung [7]. However, although effective, these aerosols contain large particles in the 5-10 µm range, as they are generated by a vibrating mesh nebulizer system [8], and will have limited penetration to the deep lung. The hypothesis of Morozov and van Hoek is that nanoaerosols enable delivery of a clinically effective outcome with a lower dose due to alveolar penetration of the nano-sized aerosol particles [9]. Morozov[10] showed that biologically active substances can be aerosolized by using electro-spray nanoaerosol generator with count median aerodynamic diameter (CMAD) in the range of 20-200 nm. Therapeutic action of thus atomized drugs shows notable difference from action of the same drug introduced via different routes. For example, the clinically effective dose of nanoaerosolized indomethacin was found to be six orders of magnitude less than the oral dose required for the same effect [11].

These concepts were further established by recent *in vivo* studies that showed efficiency of inhalation therapy by delivering nanoaerosol of the liposome encapsulated levofloxacin (LEL) in treatment of tularemia in mice caused by Francisellanovicida[12]. Francisella infection is known to be susceptible to levofloxacin [13], and liposomal ciprofloxacin was found to be an improved formulation over ciprofloxacin alone [14]. Thus, we generated nanoaerosols of liposome-encapsulated levofloxacin and used them for the therapeutic aerosol treatment of mice infected with pneumonic tularemia [12]. It required 94 times less than the oral required dose and approximately 8 times lower than the intraperitoneal dose when the LEL nanoaerosol was delivered to the diseased lung of BALB/c mice in the form of nanoaerosol (dia.<200 nm). This success opened an enthusiasm to understand how the LEL nanoaerosols get transported, disseminated and deposited inside the mouse lung.

Pulmonary drug delivery (PDD) is of significant interest due to many advantages of PDD such as (i) a large surface area of lungs (about 100 m^2) accessible to rapid absorption provided by terminal bronchioles and alveoli, (ii) a thin (0.1–0.2 mm of alveolar epithelium) physical barrier for absorption, promoting rapid uptake into the bloodstream, (iii) the absence of extreme pH, (iv) no first-pass liver metabolism as compared to oral introduction, with minimum reduction of bioavailability, (v) rich blood supply, (vi) rapid systemic delivery from alveolar region to the blood, and (vii) minimal extracellular enzyme levels for metabolic breakdown compared with the gastrointestinal tract, (viii) bypass digestive complications, extracellular enzymes and interpatient metabolic differences that result from gastrointestinal absorption [15-17]. Targeted aerosol delivery to the lung tissue may improve therapeutic efficiency and minimize unwanted side effects [9].

Despite enormous progress in optimizing aerosol delivery to the lung, targeted aerosol delivery to specific lung regions other than the large airways or the lung periphery has not been adequately achieved to date [18]. Additionally, the *in vivo* data on respiratory deposition of nanoaerosols in various regions of the mice lungs are very limited.

In order to better understand deposition patterns of nano-sized aerosols, and to resolve the issues of disparate findings from *in vivo* results it is necessary to understand the drug dosimetry. With this aim in mind, the present work employed mathematical expression based semi-empirical multiple path particle dosimetry (MPPD, version 3.0) computational tool to simulate inhaled nanoaerosol deposition. The study objectives were: 1) to predict inhaled LEL nanoaerosols deposition in various lung regions, 2) to correlate these computational results with *in vivo* experimental data, and 3) to estimate real doses obtained in treatment of mice with nanoaerosols of antibiotics.

1.1. Relevant Concepts and Theories

Mouse models are often used in studies to understand disease development, progression, and treatment. Studies showed that mouse lung airway dimensions e.g., length, cross-section significantly differ between B6C3F1 and BALB/c strains [19,20]. Total lung deposition is species dependent i.e., interspecies differences in total lung deposition may occur [21]. A decrease in total lung deposition occurs with increasing particle size. 'Respirable' size range varies animal to animal e.g., mouse strains [22].

Figure 1 depicts various regions and the asymmetric branching pattern that exist in the normal anatomy of a BALB/c mouse lung [23]. Literature defined extrathoracic (ET) or Head region (head, including nasal cavity, mouth, pharynx and larynx [24], tracheobronchial region (TB, including trachea, main and lobar bronchi, up to terminal bronchioles) [25], and pulmonary (P, including respiratory bronchioles, alveolar ducts and sacs) [26].
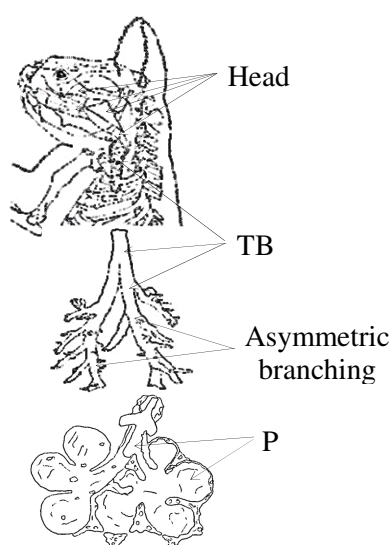
Figure 1 Asymmetric branching pattern of the BALB/c mice lung and various regions (extrathoracic (ET) or Head, tracheobronchial (TB), and pulmonary (P))

Distribution of inhaled nanoaerosols deposition in the lung airways is governed by five deposition mechanisms. They are: 1) inertial impaction, 2) Brownian diffusion, 3) gravitational settling, 4) interception, and 5) electrostatic attraction [27-29]. The respiratory deposition fraction (DF) of inhaled aerosols is dependent on the measure of DF with respect to GSD. Additionally, a bias arises if the DF of a polydisperse aerosol is utilized as a measure of DF for monodisperse aerosol or vice versa [30]. Present understanding on deposition mechanisms specific to the particular lung regions or anatomical units are: impaction and diffusion in the ET region, impaction, diffusion and sedimentation in the TB region, and diffusion and sedimentation in the P region [31].

2. MATERIALS &METHODS

Obtaining regional deposition for mouse lung through *in vivo* experiments is challenging. Computational simulation based on mathematical expressions of aerosol particles transport and deposition may provide important insight in this endeavor. The asymmetric multiple-path particle dosimetry (MPPD, version 3.0) model was adopted in this study. MPPD was originally developed by the Chemical Industry Institute for Toxicology (CIIT), Research Triangle Park, North Carolina, USA. CIIT was later acquired by the Applied Research

Associates Inc., Albuquerque, New Mexico, USA and it allows the scientific community to use this software for academic or research purposes. Its performance was verified and reported in various studies [32-33]. It is widely used in the research and regulatory science communities.

The MPPD program calculates multiple particles flow paths to multiple airways at any instant. It is a realistic model based on actual geometry of mouse lung airways by incorporating asymmetric branching pattern, and calculation is done for individual airway. Like other modeling studies the MPPD adopted 22 generation morphometry in its simulation. The model is applicable to both monodisperse and lognormally distributed polydisperse aerosols with a wide particle size range from 10 nm to 20 μm. It is able to calculate total deposition, as well as specific site of lung such as regional and lobar deposition. The deposition fraction can be plotted as a function of airway regions, generation number, various breathing patterns and particle concentrations. Deposition value is determined by using tree traversal procedure at proximal and distal ends.
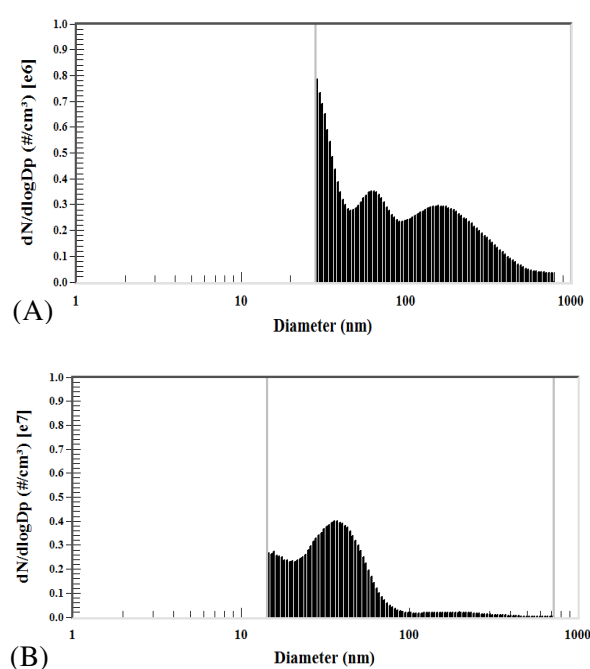
Figure 2 (A) The aerodynamic size distribution of liposome encapsulated levofloxacin (LEL) nano-aerosolized particles determined by scanning mobility particle sizer spectrometer. **(B)** Spectrum of non-encapsulated levofloxacin.

The *in vivo* experimental study involved inhalation by free-breathing mice in a whole body exposure chamber of LEL nanoaerosols for 4 hours/day and 5 days consecutively [12]. These data were used as some of the input parameters of MPPD which employs mathematical expressions of lung deposition mechanisms in computer simulation to calculate the particle dosimetry. MPPD incorporated other LEL nanoaerosol properties specifically, CMAD of 80 nm, geometric standard deviation (1.63), aerosol concentration (3,580 mg/m^3) and physiological conditions of the mouse lung such as nasal breathing rate (144.6 l/min), functional residual capacity (FRC) 0.6 ml, tidal volume (0.20 ml) and inhalability correction was also included.

Figure 2 shows the aerodynamic size distribution of the LEL nanoaerosols determined by a scanning mobility particle sizer spectrometer (TSI Inc., Shoreview, Minnesota, USA).

Deposition results were calculated as the regional (Head, TB, P) and thoracic (TB+P) fractions for the whole lung.

Furthermore, to compare with available *in vivo* information in the literature reported by Koivisto et al [34], Alessandrini et al [23], Kuehl et al [35], and Raabe et al [36], our MPPD simulation parameters for various experimental scenarios were as close as possible to the scenarios used in these studies.

3. RESULTS AND DISCUSSION

The predictive power of MPPD was demonstrated in a comprehensive study on FVBN/J mice for silver oxide nanoparticles conducted by Asgharian et al [33]. They have found a reasonable agreement when comparing predicted deposition factions with four experimental studies undertaken by Raabe et al [36] on CF1 mice; Oldham et al [37] on BALB/c mice; Kuehl et al [35] on B6C3F1 mice, and Hsieh et al [38] on C57BL/6 mice. Lung and breathing parameters in each of these studies were used in MPPD model predictions.

3.1. Fit with known data of Propst et al [12]

Simulation output shows that the nanoaerosols with aerodynamic diameter 40 nm (Figure 3) are deposited more highly in the pulmonary or respiratory region compared to TB and Head regions, where larger particles tend to deposit better.
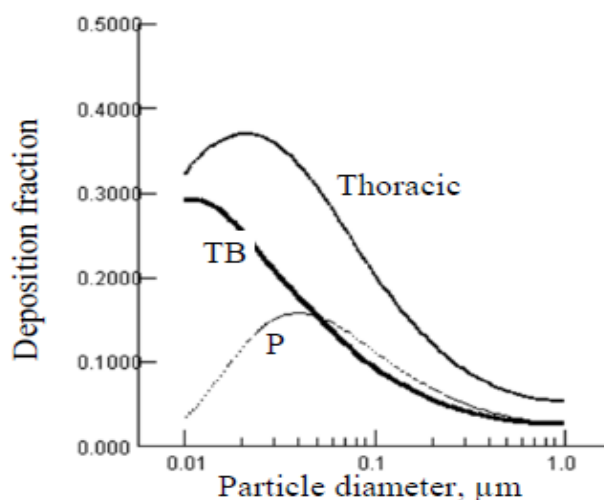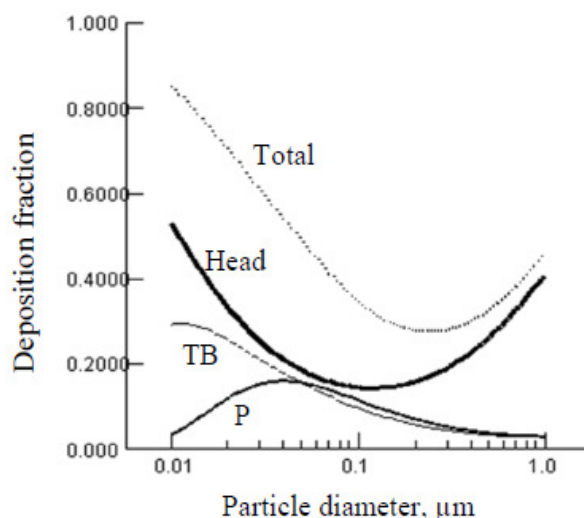

Figure 3 Comparison of deposition fraction of liposome encapsulated nanoaerosol particles in tracheobronchial (TB), pulmonary (P) and thoracic (TB+P) regions of mice lung.

The calculated deposition fraction of monodisperse aerosol in central respiratory airway is about 19% while 14% in the peripheral conducting airways. Our calculation also shows that about 37% LEL particles deposited in the lung's Head, TB and P regions combined, and the remaining portion gets exhaled. In the pulmonary region, we calculated that about 6% particles get deposited. A cross-simulation study showed that the LEL deposits 2% more than non-encapsulated levofloxacin. This phenomenon can be due to the larger size upon liposome encapsulation as seen from comparison of spectra on Figures 2A and 2B. These larger particles might experience higher impaction force while flowing through head airways.

Figure 4 shows the total predicted deposition fractions in the lung's Head, TB and P regions. The deposited mass in the pulmonary region is about 70 ng of nanoaerosols upon simulating mass fraction versus lung generation numbers. It is our understanding that these

particles would probably deliver maximum therapeutic and systemic effects in the deep lung which contains alveolar sacs.

Figure 4 Comparison of deposition fraction of liposome encapsulated nanoaerosol particles in head airway, tracheobronchial (TB), pulmonary (P) regions and total (Head + TB + P) lung of mice.

When considering a range of aerosols from nano to submicron sizes (refer to Figure 3), the LEL nanoaerosols larger than 200 nm poorly deposit in the TB and P regions but greatly deposit in the Head region which can be explained by the predominance of inertial impaction and sedimentation mechanisms combined effects.

It has been observed that the increase of submicron particle size increases Head deposition (refer to Figure 4). Moreover, nanoparticles of 10-30 nm diameter range has low tendency to deposit in the Head and TB airways but high in the P region due to high diffusivity. The 50 nm particle deposits equally in TB and P regions whereas particles with the size of 80 nm or higher poorly deposit in the TB and P regions. Inhaled particles clearance is assumed to occur primarily due to mucociliary movement inside TB regions [39]. It was noticed that irrespective of accounting for this property as simulation parameter, the depositions for various monodisperse aerosols were unaffected for Head, TB and P regions. The mass clearance in the TB region was about 10 µg/min. The model prediction of deposited mass for TB and P regions were 0.68 µg/min and 0.55 µg/min, respectively.

3.2. Fit with known data of Koivisto et al[34] and Alessandrini et al [23]

Koivisto et al [34] conducted an *in vivo* study with TiO_2 nanoaerosols (size range 10 nm to 60 nm) to determine deposition in the BALB/c/Sca mice lungs and found pulmonary deposition of 11% for a single exposure. We calculated also the pulmonary deposition taking into account size of TiO_2 nanoaerosols, and the deposition was calculated to be about 10% upon incorporating mouse's physiological characteristics as close as possible to Koivisto's study [34]. The precise parameters were: study subject BALB/c mouse, single exposure of 4 hours/day, polydisperse aerosol size range 10 nm to 60 nm with concentration of 3580 mg/m^3, nasal breathing of 144.6 l/min, FRC 0.6 ml, and tidal volume of 0.20 ml.

Alessandrini et al [23] undertook an *in vivo* experiment with BALB/c mice of 20 min exposure for 2 days, tidal volume of 0.229 ml, and minute ventilation 110 ml/min. The experimental aerosols contained iridium ultrafine particles with CMAD 35 nm, count concentration 9.8 ± 0.9 x 10^6 /cc, GSD 1.7, mass concentration 0.2 mg/m^3. In that study, the total lung deposition was estimated as 42%, of which 38% were deposited in the conducting

airways and 62% in the alveolar region [23]. The MPPD simulation performed with these input parameters predicted a total deposition of 45% where the Head, TB and P regions accounted for 37%, 27% and 36%, respectively.

3.3. Fit with known data of Kuehl et al [35]

Kuehl and other co-workers conducted an *in vivo* study with C57BL/6 mice restrained and nose-only inhalation for 4 minutes to determine regional lung deposition of radiolabeled polydisperse aerosols of 0.5, 1.0, 3.0 and 5.0 μm MMAD [35]. They have reported that the deposition patterns of aerosols between 0.5 and 5.0 μm showed an increase in overall and peripheral deposition as the particle size decreased. To compare with these data the MPPD simulation input parameters were chosen as close as possible to the Kuehl et al [35]. The precise parameters were: study subject BALB/c mouse, exposures of 4 hrs/day for 5 days, monodisperse aerosols of MMAD 0.5, 1.0, 3.0 and 5.0 μm with concentration of 3580 mg/m^3, nasal breathing of 144.6 l/min, FRC 0.6 ml, tidal volume of 0.20 ml and clearance not considered.

Table 1 Comparison between MPPD predicted liposome encapsulated nanoaerosol particles deposition in mouse lungs' various regions with *in vivo* results of Kuehl et al [35].

Particle dia. MMAD (μm)	MPPD(%)			Kuehl et al [35](%)		
	Head	TB	P	Oral/nasal	TB	P
0.5	25.6	3.8	5.6	28.6	2.0	10.7
1.0	38.1	3.1	3.8	58.0	8.2	2.2
3.0	50.2	2.2	1.9	46.6	4.7	2.3
5.0	43.5	1.3	1.2	61.7	4.5	0.2

As seen from the results presented in Table 1, the MPPD simulated data are very much agreed for the Head regional deposition whereas for the TB region, MPPD depositions is about twice as high for 0.5 μm Nanoaerosols and 50% less for 1.0, 3.0 and 5.0 μm particles deposition reported in Kuehl et al [35] work. In contrary, the MPPD deposition for the P region is about 45% less for 0.5 μm, 80% more for 1.0 μm, 24% less for 3.0 μm, and 80% more for 5. μm particles compared to Khuel's work. The possible reasons for this discrepancy between MPPD prediction and Kuehl et al [35] are: a) physiological differences in the mice strains BALB/c vs C57BL/6, b) exposure time 4 hrs per day for 5 days vs 4 min for 8 times on same day, and c) free mice in a cell filled with Nanoaerosols vs restrained and nose-only exposure to Nanoaerosols.

3.4. Fit with known data of Raabe et al [36]

Furthermore, the MPPD predicted LEL deposition in the mouse lung was compared with the data of *in vivo* study conducted by Raabe et al [36]. All the MPPD simulations' input parameters were as close as possible to the Raabe's data, and the simulation results are presented in Table 2. The precise parameters were: study subject BALB/c mouse, single exposure of 45 minutes, monodisperse aerosols of MMAD 190 nm and 767 nm with density 2.46 g/cc and GSD 1.3, nasal breathing frequency 160/min, FRC 0.6 ml, and tidal volume of 0.20 ml. In order to comply with MPPD's acceptable unit for input particle size (aerodynamic diameter), we converted Raabe at al [36] reported aerodynamic resistance diameters 0.270 μm and 1.09 μm into aerodynamic diameters of 190 nm and 767 nm, respectively.

Table 2 Comparison between MPPD predicted liposome encapsulated nanoaerosol particles deposition in mouse lungs' various regions with *in vivo* results of Raabe et al [36].

Particle dia. MMAD (nm)	MPPD (%)		Raabe et al [36] (%)	
	TB	P	TB	P
190	7.82	12.37	14.48	45.4
767	2.00	2.73	6.08	9.7

Here the MPPD predicted TB and P deposition fractions are differed (TB, 50% and P, 75%) (refer to Table 2) from the reported experimental data of Raabe et al [36]. The possible explanations of these variations can be: a) MPPD is a semi-empirical mouse deposition model of BALB/c mice whereas Raabe's experiment was on CFI mice, airway dimensional parameters differ between both species; b) MPPD adopted TB morphometry lung cast CT-scan data to establish airway dimensional parameters [33]; c) MPPD predicts upper respiratory tract (includes TB) deposition due to impaction and lower respiratory tract (includes P) deposition due to impaction and gravitational settling [33], there could be unaccounted parameters such as Brownian diffusion, interception and electrostatic charge force which could be affecting the *in vivo* experiment, and d) Raabe's experimental mice were restrained and only their noses were exposed to the aerosols whereas MPPD simulates free nasal breathing with whole body exposure to the experimental aerosol.

4. CONCLUSIONS

Although, there is no *in vivo* experimental data available on regional level deposition for LEL therapeutic nanoaerosols in mouse lungs, this work computationally (*in silico*) predicted the dosimetry information by employing the semi-empirical MPPD model. The MPPD model prediction compared favorably and closely with several *in vivo* experimental studies on other mouse strains. This work will open the scope for further studies to determine appropriate particle sizes of other inhalable antibiotics to produce the appropriate dose for target regions of the lung, and for the use of MPPD to model the deposition of nanoaerosols.

ACKNOWLEDGEMENT

DISCLAIMER

The views and opinions expressed in this article are those of the authors and do not necessarily reflect the official policy or position of any agency of the U.S. government entity.

REFERENCES

[1]   Borm, P.J., Robbins, D., Haubold, S., Kuhlbusch, T., Fissan, H., Donaldson, K., Schins, R., Stone, V., Kreyling, W., Lademann, J., Krutmann, J., Warheit, D., and Oberdoster, E. The Potential Risks of Nanomaterials: A Review Carried out for ECETOC. *Particle Fiber and Toxicology,* 3, 2006, pp. 11-20.

[2]   Oberdorster, G. 2007. Toxicology of Nanoparticles: A Historical Perspective. *Nanotoxicology*. **1**, 2007, PP. 1-25.

[3]   Xia, T., Kovochich, M., Liong, M., Meng, H., Kabehie, S., Zink, J.I., and Nel, A.E. Polyethyleneimine Coating Enhances the Cellular Uptake of Mesoporous Silica Nanoparticles and Allows Safe Delivery of siRNA and DNA Constructs. *ACS Nano*, **3**, 2009, pp. 3273–3286.

[4]   Cohen, J.M., Teeguarden, J.G., and Demokritou, P. An Integrated Approach for the In-vitro Dosimetry of Engineered Nanomaterials, *Particle Fiber and Toxicology,* **11**, 2014, pp. 1-12.

[5]   Borm, P.J. Particle Toxicology: from Coal Mining to nanotechnology. *Inhalation Toxicology,* **14**, 2002, pp. 311-324.

[6]   Nel, A.E., Madler, L., Velegol, D., Xia, T., Hoek, E.M.,Somasundaran, P., Klaessig, F., Castranova, V., and Thompson, M. Understanding Biophysicochemical Interactions at the Nano-bio Interface. *Nature Materials,* **8**, 2009, pp. 543–557.

[7]   Clancy, J.P., Dupont, L., Konstan, M.W., Billings, J., Fustik, S., and Goss, C.H. Phase II Studies of Nebulised Arikace in CF Patients with Pseudomonas Aeruginosa Infection. *Thorax*, **68**, 2013, pp. 818-825.

[8]   Martin, A.R., Gleske, J., Katz, I.M., Hartmann, M., Mullinger, B., Haussermann, S., Caillibotte, G., and Scheuch, G. Laser Diffraction Characterization of Droplet Size Distributions Produced by Vibrating Mesh Nebulization in Air and a Helium–oxygen Mixture. *Journal of Aerosol Science,* **41**, 2010, pp. 1159-1166.

[9]   Morozov, V.N., Kanev, I.L., Mikheev, A.Y., Shlyapnikova, E.A., Shlyapnikov, Y.M., Nikitin, M.P., Nikitin, P.I., Nwabueze, A.O., and van Hoek, M.L. Generation and Delivery of Nanoaerosols from Biological and Biologically Active Substances. *Journal of Aerosol Science,* **69**, 2014, pp. 48-61.

[10]   Morozov, V.N. Generation of Biologically Active Nano-aerosol by an Electrospray-neutralization Method. *Journal of Aerosol Science,* **42**, 2011, pp. 341-354.

[11]   Onischuk, A.A., Tolstikova, T.G., Sorokina, I.V., Zhukova, N.A., Baklanov, A.M., Karasev, V.V., Dultseva, G.G., Boldyrev, V.V., and Fomin, V.M. Anti-inflammatory Effect from Indomethacin Nanoparticles Inhaled by Male Mice. *Journal of Aerosol Medicine and Pulmonary Drug Delivery,* **21**, 2008, pp. 231-243.

[12]   Propsti, C.N., Nwabueze, A.O., Kanev, I.L., Pepin, R.E., Gutting, B.W., Morozov, V.N., and van Hoek, M.L. NanoaerosolReduce Required Effective Dose of Liposomal Levofloxacin Against Pulmonary Murine Francisella Tulerensis Subsp. Novicida Infection. *Journal of Nanobiotechnology*, **14**, 2016a, pp. 29-39.

[13]   Propst, C.N., Pylypko, S.L., Blower, R.J., Ahmad, S., Mansoor, M., and van Hoek, M.L. Francisellaphilomiragia infection and lethality in mammalian tissue culture cell models, Galleria mellonella, and BALB/c mice. *Frontiers in Microbiology*, **7**, 2016b, pp. 696(1-10).

[14]   Hamblin, K.A., Armstrong, S.J., Barnes, K.B., Davies, C., Wong, J.P., et al. Liposome Encapsulation of Ciprofloxacin Improves Protection Against Highly Virulent Francisella Tularensis Strain Schu S4. *Antimicrobial Agents and Chemotherapy*. **58**, 2014, pp. 3053-3059.

[15]   Labiris, N.R., and Dolovich, M.B. Pulmonary Drug Delivery. Part I: Physiological Factors Affecting Therapeutic Effectiveness of Aerosolized Medications. *British Journal of Clinical Pharmacology*. **56**, 2003, pp. 588–599.

[16]   Sanders M. Inhalation Therapy: an Historical Review. *Primary Care Respiratory Journal*. **16**, 2007, pp. 71–81.

[17]   Brillault, J., Tewes, F., Couet, W., and Olivier, J.C. In-vitro Biopharmaceutical Evaluation of Ciprofloxacin/metal Cation Complexes for Pulmonary Administration, *European Journal of Pharmaceutical Science*, **97**, 2017, pp. 92-98.

[18]   Darquenne, C., Fleming, J.S., Katz, I., Martin, A.R., Schroeter. J., Usmani, O.S., Venegas, J., and Schmid, O. Bridging the Gap between Science and Clinical Efficacy: Physiology, Imaging, and Modeling of Aerosols in the Lung, *Journal of Aerosol Medicine and Pulmonary Drug Delivery,* **29**, 2016, pp. 107-126.

[19]   Oldham, M.J., and Robinson, R.J. Dosimetry Predictions in an Animal Model of Emphysema, *The Anatomical Record,* **290**, 2007, pp. 1309–1314.

[20]   Thiesse, J., Namati, E., Sieren, J.C., Smith, A.R., Reinhardt, J.M., Hoffman, E.A., and McLennan, G. Lung Structure Phenotype Variation in Inbred Mouse Strains Revealed Through In-vivo Micro-CT Imaging, *Journal of Applied Physiol*ogy, **109**, 2010., pp. 1960–1968.

[21]   Hoyt, R.F., Hawkins, J.V., Kennett,and M.J.Mouse Physiology. In: Fox, J.G., Barthold, S.W., Davisson, M.T., Newcomer, C.E., Quimby, F.W., and Smith, A.L., Eds.,TheMouse in Biomedical Research. vol. III Normative Biology, Husbandry, and Models. New York: Elsevier, 2007, pp.23-90.

[22]   Thomas, R.J. Particle Size and Pathogenicity in the Respiratory Tract. *Virulence*, **8**, 2013, pp. 847-858.

[23]   Alessandrini, F., Semmler-Behnke, M., Jakob, T., Schulz, H., Behrendt, H.and Kreyling W. Total and Regional Deposition of Ultrafine Particles in a Mouse Model of Allergic Inflammation of the Lung. *Inhalation Toxicology,* **20**, 2008, pp. 585–593.

[24]   Gross, G.J., Soucy, P., Martin, D.J., D'Alton, M., and Carpenter, B.F. Extrathoracic Pulmonary Sequestration Detected by Antenatal Ultrasonography. *Pediatric Surgery International*. **7**, 1992, pp. 382-383.

[25]   Newton, P.E., Wooding, W.L., Bolte, H.F., Derelanko, M.J., Hardisty, J.F., and Rinehart, W.E. A Chronic Inhalation Toxicity/Oncogenicity study of Methylethylketoxime in Rats and Mice. *Inhalation Toxicology,* **13**, 2001, pp. 1093-1116.

[26]   Phalen, R.F. Inhalation Studies: Foundations and Techniques.2nd Edition. New York: Informa Healthcare, 2009, pp. 187-214.

[27]   Hinds, W.C. Aerosol Technology: Properties, Behavior, and Measurement of Airborne Particles. 2nd Edition. New York: Wiley-Interscience. 1999, pp. 235.

[28]   Finlay, W.H. Lung Deposition Simulation.In: Hickey, A.J., Ed., Pharmaceutical Inhalation Aerosol Technology. New York: Informa, 2004, pp. 155-171.

[29]   Ali, M. Pulmonary Drug Delivery. In: Kulkarni, K, Ed., Handbook of Non-invasive Drug Delivery Systems. Amsterdam, The Netherlands: Elsevier; 2009, pp. 209-246.

[30]   Londhal, J., Moller, W., Pagels, J.H., Kreyling, W.G., Swietlicki, E., and Schmid, O. 2013. Measurement Technique for Respiratory Tract Deposition of Airborne Nanoparticles: ACritical Review. *Journal of Aerosol Medicine and Pulmonary Drug Delivery*, **26**, 2013, pp. 1-26.

[31]   Mendez, L.B., Gookin, G., and Phalen, R.F. Inhaled aerosol particle dosimetry in mice: a review. *Inhalation Toxicology,* **22**, 2010, pp. 15-20.

[32]   Asgharian, B., Hofman, W., and Bergmann, R. Particle Deposition in a Multiple-path Model of the Human Lung. *Aerosol Science and Technology*, **34**, 2001, pp. 332-339.

[33] Asgharian, B., Price, O.T, Oldham, M, Chen, L.C., Saunders, E.L., Gordon, T., Mikheev. V.B., Minard. K.R., and Teeguarden. J.G. Computational Modeling of Nanoscale and Microscale Particle Deposition, Retention and Dosimetry in the Mouse Respiratory Tract. *Inhalation Toxicology,* **26**, 2014, pp. 829–842.

[34] Koivisto, A.J., Makinen, M., Rossi, E.M., Lindburg,H.K., Miettinen, M., Falck, G.C.M., Norppa, H., Alenius, H., Korpi, A., Riikonen, J., et al. Aerosol Characterization and Lung Deposition of Synthesized TiO_2 Nanoparticles for Murine Inhalation Studies. *Journal of Nanoparticle Research*, **13**, 2011, pp. 2949-2961.

[35] Kuehl, P.J., Anderson, T.L., Candelaria, G., Gershman, B., Harlin, K., Hesterman, J.Y., Holmes, T., Hoppin, J., Lackas, C., Norenberg, J.P., et al. Regional Particle Size Dependent Deposition of Inhaled Aerosols in Rats and Mice. *Inhalation Toxicology,* **24,** 2012, pp. 27-35.

[36] Raabe, O.G., Al-Bayati, M.A., Teague, S.V., Rosalt A. Regional Deposition of Inhaled Monodisperse Coarse and Fine Particles in Small Laboratory Animals. *The Annals of Occupational Hygiene*, **32**, 1988, pp. 53-63.

[37] Oldham, M.J., Phalen, R.F., and Budiman, T. Comparison of Predicted and Experimentally Measured Aerosol Deposition Efficiency in BALB/C Mice in a New Nose-only Exposure System. *Aerosol Science and Technology,* **43**, 2009. pp. 970–977.

[38] Hsieh, T.H., Yu, C.P., and Oberdorster, G. 1999. Deposition and Clearance Models of Ni Compounds in the Mouse Lung and Comparisons with the Rat Models. *Aerosol Science and Technology*, **31**, 1999, pp. 358-372.

[39] Mall, M., Grubb, B.R., Harkema, J.R., O'Neal, W.K., and Boucher, R.C. Increased Airway Epithelial Na+ Absorption Produces Cystic Fibrosis-like Lung Disease in Mice. *Nature Medicine*, **10**, 2004, pp. 487-493.